

Traffic Modeling of a Cooperative Charge While Driving System in a Freight Transport Scenario

*Original*

Traffic Modeling of a Cooperative Charge While Driving System in a Freight Transport Scenario / Deflorio, FRANCESCO PAOLO; Castello, Luca. - In: TRANSPORTATION RESEARCH PROCEDIA. - ISSN 2352-1465. - ELETTRONICO. - 6:(2015), pp. 325-350. (Intervento presentato al convegno 4th International Symposium of Transport Simulation-ISTS'14 tenutosi a Ajaccio, France nel 1-4 giugno 2014) [10.1016/j.trpro.2015.03.025].

*Availability:*

This version is available at: 11583/2561810 since:

*Publisher:*

ELSEVIER

*Published*

DOI:10.1016/j.trpro.2015.03.025

*Terms of use:*

This article is made available under terms and conditions as specified in the corresponding bibliographic description in the repository

*Publisher copyright*

(Article begins on next page)

4th International Symposium of Transport Simulation-ISTS'14, 1-4 June 2014, Corsica, France

## Traffic Modeling of a Cooperative Charge While Driving System in a Freight Transport Scenario

Francesco Deflorio<sup>a</sup> \*, Luca Castello<sup>a</sup>

<sup>a</sup>DIATI, Politecnico di Torino, corso Duca degli Abruzzi 24, 10129 Torino, Italy

---

### Abstract

The aim of this paper is to present a research study on a traffic model developed for analysing the performance of the wireless inductive systems for charging while driving (CWD) fully electric vehicles (FEVs) from both traffic and energy points of view.

The design assumptions of the developed traffic model are aimed to simulate in particular a freight distribution service in a fully cooperative traffic environment. In this case, the CWD service could be used to guarantee the minimum state of charge (SOC) of the batteries at the arrival to the depot that allows the vehicles to shortly start with further activities. In this way, the fleet manager could avoid wasting time for the stationary recharge, thus increasing the level of service of the freight distribution.

The CWD system is applied to a multilane ring road with several intermediate on-ramp entrances, where the slowest lane is reserved for the dynamic charging activities, when authorized vehicles are present. A specific traffic model has been developed and implemented adopting a mesoscopic approach, where vehicle energy needs and charging opportunities affect drivers' behavior. Overtaking maneuvers, as well as new entries in the CWD lane of vehicles that need to charge, have been modeled by taking into account a fully cooperative driving system among vehicles which manages adequate gaps between consecutive vehicles. Finally, a speed control strategy in which vehicles can be delayed to create an empty time-space slot in the CWD lane, is simulated at a defined node. This type of control, though is simulated to allow extraordinary maintenance operations, which may require a free charging zone for a given time slot, could also be applied to support merging maneuvers for on ramp vehicles.

© 2015 The Authors. Published by Elsevier B.V. This is an open access article under the CC BY-NC-ND license

(<http://creativecommons.org/licenses/by-nc-nd/4.0/>).

Selection and/or peer-review under responsibility of the Organizing Committee of ISTS'14

*Keywords:* Charging While Driving; traffic simulation; multi-lane road modeling; electric freight vehicles

---

---

\* Corresponding author. Tel.: +39-011-0905601; fax: +39-011-0905699.

E-mail address: [francesco.deflorio@polito.it](mailto:francesco.deflorio@polito.it)

## 1. Introduction

The majority of fully electric vehicles (FEVs) currently satisfies the electric energy needs for motion with an on-board battery. The extensive literature on FEVs includes discussions of the following: battery problems particularly concerning limitations in size and power, their weight, life and recharge time and the lack of charging points. These problems are even more relevant for freight distribution services, where the masses and the distances travelled are relevant and where the stationary recharge would require many charging stations. However, electric vehicles could represent one of the possible solutions to low air pollutants emissions in the city centers, where a freight distribution service often has to deliver. For this reason, the charge while driving (CWD) system could represent a technology to contain the batteries sizes and the recharging infrastructures costs without impacting on the vehicles autonomy.

In particular, Boulanger et al. (2011) analysed the problems related to battery charging management, the uncertainty surrounding the monitoring of the state of charge (SOC), the limited availability of charging infrastructure and the long time required to recharge; problems that have generated range anxiety. The use of intelligent transport systems (ITS), in particular vehicle to vehicle or to infrastructure (V2X) communications, was evaluated to allow drivers to accurately and confidently locate charging stations where they could recharge the battery in the shortest amount of time (Ezell, 2010). Johnson et al. (2013) evaluated how connected vehicle technologies can facilitate the rapid charging of FEVs at charging stations throughout the road network. The market acceptance of FEVs, travel needs and consumer choices, particularly for the first car in the household, were also analysed by Kirsch (2000). Moreover, extensive research has claimed that the challenges of battery inefficiency and the large and wasted space in the FEVs can be overcome by the wireless power transfer (WPT) technology. This technology electrically conducts energy from a source to an electric device without any interconnecting mediums (Palakon et al, 2011). Finally, another important element that supports a battery charging modality with frequent and low energy transfer while driving is that the SOC must be managed carefully and the batteries should never be fully discharged to avoid an excessive shortening of the battery life cycle.

The aim of this research study is to provide a method to support preliminary studies about one of the possible future technology that could contribute to use FEVs in freight transport. One of the goals of the European white paper is to achieve essentially CO<sub>2</sub>-free city logistics in major urban centers by 2030 and CWD technology could represent one of the possible ways to reach this target. The model can simulate the performance of the wireless inductive charge of the electric vehicles while driving, from both traffic and energy points of view. Beginning with an electric vehicle supply equipment (EVSE) layout defined and analysed in a previous study (Deflorio et al, 2013), a model for the traffic flow simulation is implemented to quantify and describe traffic performance, useful for drivers and operators, but also the electric power that should be provided by an energy supplier for a proper management of the charging system.

## 2. The CWD service for freight vehicles and the technological scenario

The following paragraphs are aimed at providing a brief overview on how a CWD service based on assumptions and system requirements defined in the eCo-FEV project (2013) operates.

A driver who wants to use the CWD service should send a request, even automatically, to the charging station operator through an on-board unit (OBU). After the verification of operational requirements, the charging station operator returns the confirmation message to the user and updates the list of authorized vehicles, while the driver receives the authentication on the OBU. The CWD system should include some enforcement functions to prevent unauthorized vehicles from using the reserved lane. The position of each authorized vehicle is monitored along the CWD lane to switch on only the coils under the vehicles, thus avoiding energy wasting. The correct position monitoring is important also for vehicles outside the CWD lane because they affect overtaking maneuvers. The service should consider different classes of vehicles, according to their energy needs. Different speeds should therefore be admitted in the CWD lane and overtaking maneuvers should be managed according to a cooperative system among vehicles: advanced driver assistance systems (ADAS) guide drivers during their maneuvers and the cooperative system eventually intervenes on vehicle speeds to maintain the required gaps in the vehicle flow. This technology could serve both passenger vehicles – private or public – and freight vehicles for distribution services, on which this paper is focused.

The chosen example of freight distribution service starts from a depot quite close to the city center and connected to the motorway network by the ring road. The primary actors involved in the delivery use case (Fig. 1) can be described as:

- **FEV-Private:** it is an electric powered vehicle which provides to the ITS system its level of autonomy as well as other in-vehicle information;
- **Charging station operator:** it is the operator that provides charging services to FEVs and manages the EVSE. This operator provides also traffic information in the inductive charging lanes. If necessary, it offers booking and payment facilities;
- **Fleet operator drivers:** they drive FEVs of the fleet and are usually provided with an established delivery schedule;
- **Info operator:** this operator monitors and manages the road traffic and/or road side infrastructure systems. It provides information on traffic conditions and events (accidents, road works, road diversions, traffic restrictions, etc.). It may refer to an urban traffic management center or a highway operator.

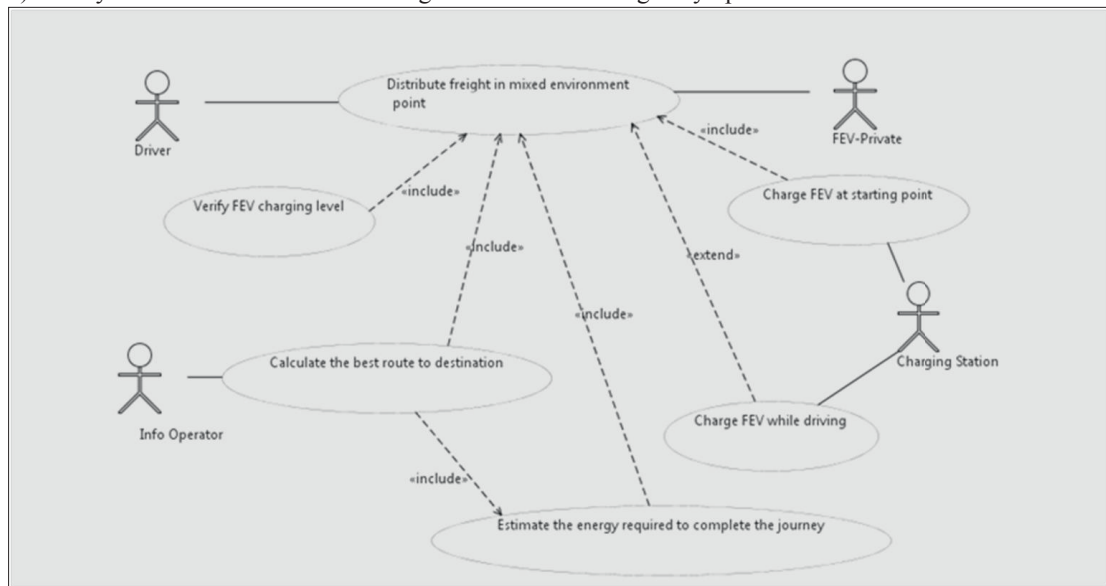


Fig. 1. Example of a use case diagram for a freight distribution service with FEV.

The CWD is here supposed to be installed only along the right-hand lane of the ring road because that lane is generally used by slower vehicles (Fig. 2). The EVSE includes inductive coils placed under the pavement surface, forming different charging zones (CZs) at a relative distance ( $l$ ). An authorized FEV that crosses the CZ couples to its high frequency alternating magnetic field and the power is transferred to charge the battery.

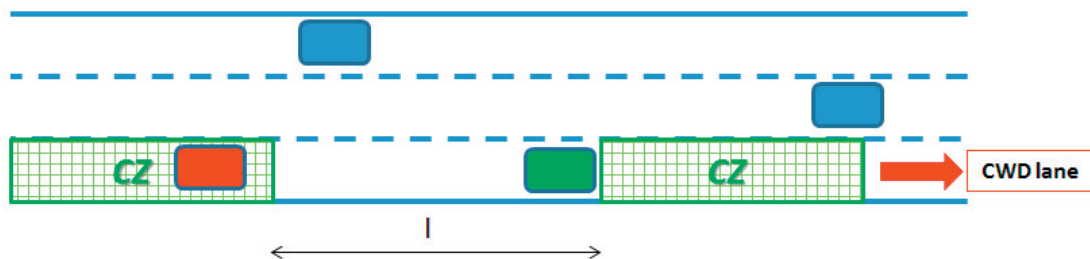


Fig. 2. CWD system layout.

### 3. The choice of the traffic model

The presented methodology refers to a freight distribution service in a near future mobility scenario, where vehicles motion could be less influenced by driver decisions. In particular, the rules that manage the vehicle behavior are here developed according to a fully cooperative system where ADAS operate both on longitudinal vehicle behavior - by speed control functions - and lateral vehicle behavior - by lane selection functions -.

The choice of the traffic modeling is derived from two primary requirements of the CWD system (eCo-FEV, 2013):

- CWD is supposed to be installed only along the right-hand lane of the ring road because that lane is generally used by slower vehicles: the traffic model must consider the disaggregation of traffic data per lane;
- CWD can be used by vehicles with different charging needs and speeds: the traffic model must consider different classes of vehicles, related to their electric charge level.

An extensive review of traffic modeling approaches can be found in Hoogendoorn and Bovy (2001). Macroscopic models are not adequate to describe this type of problem because they lose the single vehicle information and describe the mean behavior of the traffic flow on a road section. One possible approach to effectively model multilane and multiclass problems could be microsimulation, where single vehicle trajectories and interactions are modeled with a small time step resolution. A microsimulation model application example is reported by Barceló et al. (2005). Although the microsimulation approach meets the principal requirements of the traffic model for CWD, it does not model vehicle behavior according to energy needs. The current SOC of the vehicles influence drivers' decisions concerning lane changing behavior, i.e., vehicles try to enter or exit the CWD lane according to their needs. Therefore, specific rules must be defined to obtain useful results from the traffic model.

In addition, the detailed rules implemented in a microsimulation model usually require an accurate calibration process, aimed at replicating the actual driver behavior in traffic. However, currently the CWD system has been installed only in small test sites and, unfortunately, there are no opportunities to observe driver behavior in large-scale systems. Furthermore, even fully cooperative driving systems are not completely deployed. The most similar case in an actual traffic scenario can be observed in long road tunnels in which vehicle spacing or headway greater than a predefined threshold should be maintained and all vehicles travel in a predefined speed range for safety reasons (e.g. the Mont Blanc tunnel). In such systems, the vehicle behavior is controlled by safety constraints, as in the CWD model, although there are no interactions between vehicles, such as overtaking maneuvers and new entries along the lane. Furthermore, the CWD technological environment may expand only in the future, involving another generation of vehicles in which V2V will be used and many cooperative functions will be activated to facilitate the drive. An example of a cooperative scenario in highway automation system is reported in Fig. 3.

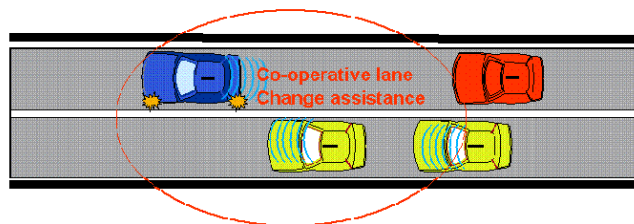


Fig. 3. Cooperative lane change assistance use case [source: ETSI, 2011].

In such a system, the observation of the current drivers' behavior is not relevant to model the traffic because vehicle motions and interactions depend more on the activated functions of the ADAS system than on drivers' decisions. A calibration process based on empirical observations of the current traffic would be compromised whenever ADAS and full cooperative systems were considered, because they affect driving and traffic behaviors.

Consequently, a mesoscopic approach would be more appropriate to model the problem because it represents a good compromise between the detailed resolution of the microscopic simulation and the current preliminary stage of development of the CWD technology. A framework of mesoscopic traffic models can be found in Cascetta (2001), whereas a recent application is proposed by Ben-Akiva et al. (2012).

#### 4. The structure of the CWD simulation model

The developed model represents the road infrastructure as a sequence of road segments - in the following indicated as “sections” - delimited by “nodes” or “detection points”. Detailed traffic information is updated only at nodes based on traffic information determined at upstream nodes. Therefore, the iterative algorithm assumes that traffic conditions along the infrastructure can be described knowing only the data related to consecutive points whose spacing, typically hundreds of meters, can be set according to the specific requirements of the analysis or of the infrastructure. The vehicle time information is defined only at nodes, also with respect to new entries of vehicles in the infrastructure. The model reproduces single vehicle trajectories without introducing a detailed time-space resolution of the driving behavior and it determines aggregated traffic information, such as vehicle counting, average headways, delays and the number of overtaking maneuvers along the CWD lane for any road section. The logic scheme adopted for two consecutive nodes is reported in Fig. 4.

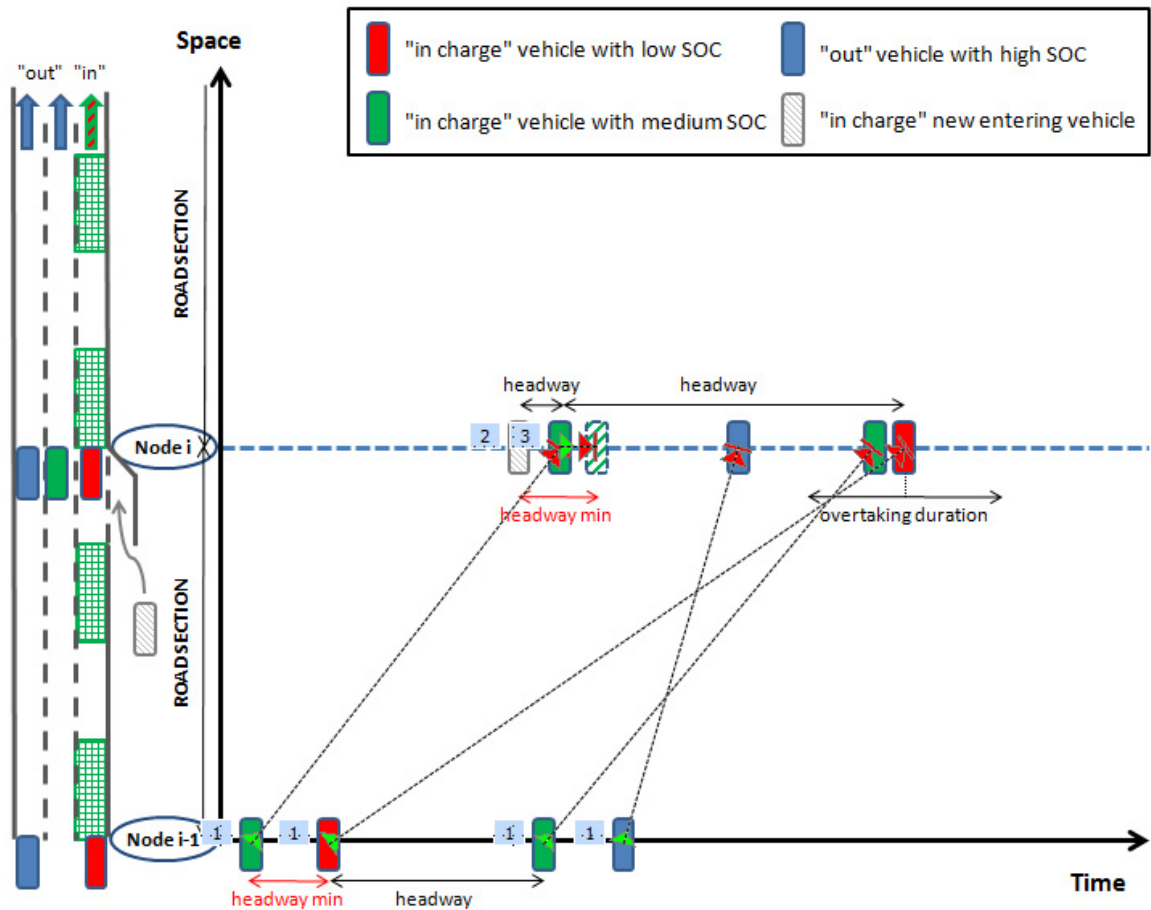


Fig. 4. Modeling of vehicle trajectories and possible interactions for two nodes.

Initially, the model estimates the arrival time of each vehicle at node (i) based on its arrival time at node (i-1) and its speed that depends on the vehicle class. Then, it manages interactions between vehicles caused by new entries in the CWD lane or by overtaking maneuvers.

Overtaking maneuvers that occur on the node are identified because the faster vehicle is not physically in the CWD lane and an erroneous vehicle count would lead to an overestimation of the energy required by the CZ on the samenode. Overtaking maneuvers are managed according to a cooperative driving model at constant speed and vehicles do not recharge while they are outside the dynamic charging lane.

New vehicles in the CWD lane are caused by new entries in the infrastructure, as represented in Fig. 4, or by “out” vehicles that move into the CWD lane. New entries can cause erroneous relative positioning between vehicles: if the headway between two vehicles is less than the minimum admissible headway (headway min), the algorithm corrects the arrival time of the following vehicle by slowing it down. In fact, due to safety and maybe technical reasons, headways less than a threshold value between two vehicles in the CWD lane may not be allowed. Also the entries in the CWD lane are managed according to a cooperative behavior: each vehicle that needs to recharge its battery is moved into the CWD lane at node, creating the eventual necessary gap in the vehicles flow by slowing down the following vehicles. The headway verification and correction is therefore performed only at discrete space steps, according to the mesoscopic modeling of vehicle behavior. In an actual scenario, this process can be managed by drivers or by the cooperative system adapting the vehicle speed along the entire section before the node where the headway adjustment is performed.

The battery SOC, monitored along the road at each node, plays a crucial role because it influences drivers' decisions whether to use the CWD service or not according to their destinations. For the analyzed freight distribution service, this process can be simplified because all the vehicles have the identical destination and the decision about charging does not depend on drivers, but on the fleet operator. Indeed, to restart the delivery operations in the second part of the day, all the vehicles of the fleet may require an energy level adequate for their operations. Vehicle SOC is also the parameter used to divide vehicles into different speed classes, according to their recharging needs.

Finally, the algorithm allows the implementation of a speed control strategy, in which vehicles can be slowed down to create an empty time-space slot in the CWD lane at a defined node. An example of this application is described by Sun and Chen (2013). This type of control could be applied to support operations that require a free CZ for a given time slot, as extraordinary maintenance activities of the coils for example. This strategy could be applied even to support merging maneuvers for vehicles entering from the secondary accesses.

#### 4.1. The model structure

The traffic simulator has been implemented using Visual Basic for Applications (VBA). It is composed of several sub routines that will be described in detail in the following paragraphs. The algorithm operates according to the functional scheme reported in Fig. 5: it generates an initial traffic state, modeled by a set of vehicles, and then it iteratively analyses travel times and energy parameters of all the simulated vehicles node by node. The routine “Strategy detection” runs only if the strategy is activated. Table 1 and Table 2 collect all input parameters required by the algorithm with the values used in simulations.

##### 4.1.1. Initial traffic state

The “Initial traffic state” routine operates according to two different approaches: the first one refers to the initial node (node 0) whereas the other to the secondary accesses.

At node 0, it calculates the maximum speed that the considered FEV can reach: it is the speed at which the resistance to motion is equal to the maximum power that the FEV engine can provide. The maximum speed is estimated by an iterative process which progressively reduces the speed by steps, starting from the road speed limit.

The maximum speed of FEVs is then assumed as FEVs free flow speed ( $v_0$ ) and it is used to estimate the average speed ( $v$ ) in the unequipped lanes (“out” vehicles), according to the Northwestern speed-density model (Drake et al. 1967):

$$v = v_0 \cdot \exp \left[ -\frac{1}{2} \left( \frac{k}{k_0} \right)^2 \right] \quad (1)$$

In this simple and reliable traffic model - within the density range used -  $k$  and  $k_0$  are respectively average and optimum densities. The relationship between the traffic flow parameters allows to estimate the average entering flow and consequently the average headway between vehicles. Subsequently, the routine progressively generates the initial headway of each couple of vehicles using a random algorithm according to the mean value and the standard

deviation of the random distribution (Daganzo, 1995). Headways are then used to calculate vehicle entering times. Using a similar random algorithm, the routine assigns each vehicle its SOC; the SOC random distribution is limited at the lower end by positive values and at the upper end by the battery size. According to the generated SOC and to the introduced SOC thresholds, the routine defines position (“out” or “in”), status (“no charge”, “charge” or “emer”) and speed of each vehicle.

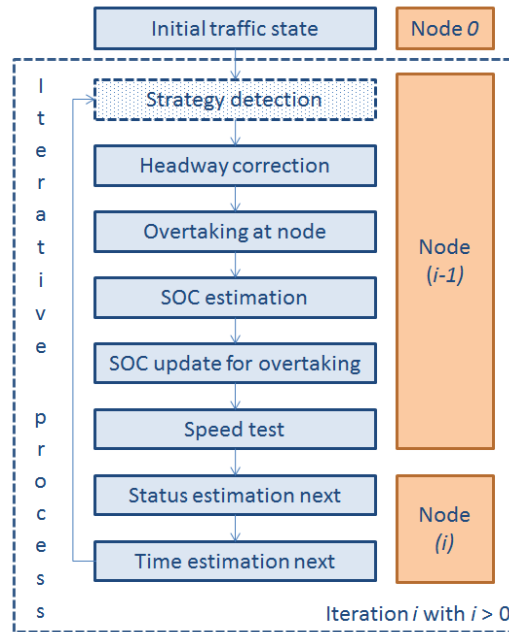


Fig. 5. Algorithm structure.

Concerning the on ramps along the ring road, the routine receives the node in which each access is located, the number of entering vehicles and, for sake of simplicity, the time window in which the entries are included as inputs. Through a uniform distribution, the routine then assigns to each vehicle an entering time included in the time window, while it sets the vehicle entering SOC according to the random algorithm used for vehicles at node 0.

4.1.2. Strategy detection

The “Strategy detection” routine operates if the strategy is active and only at the iteration corresponding to the node in which the strategy acts (briefly indicated as strategy node). It sorts the vehicle arrival times in ascending order and it selects the first vehicle whose arrival time is included in the strategy time window. The selected vehicle is then slowed down till its arrival time is equal to the strategy end time. Its average speed in the section approaching the strategy node is then evaluated to estimate the minimum headway that prevents two following vehicles from overlapping (overlap headway). Following vehicles will be subsequently managed according to “Headway correction” and “Time estimation next” routines, as explained in the next paragraphs.

4.1.3. Headway correction

The “Headway correction” routine calculates the headways between vehicles in the CWD lane and it compares them to the minimum technical headway. Unfeasible headways for CWD can be generated by entering maneuvers: if the headway between two vehicles is less than the acceptable limit, the routine corrects the arrival time of the following vehicle at the detection point by slowing it down.

If the strategy is active, its duration considerably affects vehicle speed reductions. For low speed values, the minimum technical headway in the CWD lane could be no longer adequate to guarantee the safety gap between two following vehicles. The time required to a vehicle to cover its length plus the safety spacing could be higher than the



technical headway defined for operative speeds in the CWD lane. For this reason, the routine compares the technical headway to the overlap headway previously defined: the minimum headway allowed on the strategy node is the bigger between those two values. This headway regulation is applied to the time window comprised between the initial time of the strategy and the end queue time, that is the time in which the propagation of the strategy effects, in terms of vehicle platooning, are supposed to be ended, according to the calculations developed for the considered node by the “Time estimation next” routine.

For each simulated vehicle, the “Headway correction” routine also evaluates other parameters which can be used for internal checks, such as IDs of the previous and the following vehicles and the headway with the following vehicle.

#### 4.1.4. Overtaking at node

The “Overtaking at node” routine identifies vehicles that are overtaking at detection points. The routine analyses couples of vehicles with different speeds. If the headway between these vehicles is less than half of the overtaking maneuver duration, the faster vehicle is identified as overtaking. This function is useful to detect vehicles only if they actually cross a detection point in the CWD lane: in this way, more realistic time profiles of the energy that should be provided by the electric line on CZs are obtained. The implemented overtaking model refers to an overtaking maneuver at constant speed developed in three phases: 1) lane changing from CWD lane, 2) overtaking of the slower vehicle, 3) lane changing to CWD lane. The durations of the first and third phases are assumed equal to 4 s, according to the prescriptions of the Italian technical standards for the design of road infrastructures (DM. 6792/2001). This value is also supported by Farah researches (2010, 2013). The second phase duration is the time required to cover the length of the two vehicles at a speed equal to the difference between average speeds of vehicles.

#### 4.1.5. SOC estimation

The “SOC estimation” routine firstly calculates the actual average speed of each vehicle along the last section after slowdowns generated by headway corrections. The actual average speed is used to update the SOC level of each vehicle by estimating the energy balance between consumption related to motion and the energy provided by the coils in the CWD lane.

The implemented model for estimating the vehicle energy consumption is based on the resistance to motion. The total resistance ( $R_{tot}$ ) is given by the following relationship:

$$R_{tot} = R_{drag} + R_{rolling} + R_{acceleration} + R_{slope} \quad (2)$$

Where:

$$R_{drag} = \frac{1}{2} \cdot \rho \cdot c_x \cdot A \cdot S^2 \quad (3)$$

$$R_{rolling} = m \cdot (f_0 + f_2 \cdot v^2) \quad (4)$$

$$R_{acceleration} = m \cdot a \quad (5)$$

$$R_{slope} = m \cdot g \cdot p \quad (6)$$

Therefore, the total resistance depends on the following parameters: air density ( $\rho$ ) [ $\text{kg}/\text{m}^3$ ], drag coefficient of the vehicle ( $c_x$ ), cross sectional area of the vehicle ( $A$ ) [ $\text{m}^2$ ], vehicle speed relative to the air ( $S$ ) [ $\text{m}/\text{s}$ ], vehicle mass ( $m$ ) [ $\text{kg}$ ], rolling coefficients ( $f_0$ ,  $f_2$ ) [ $\text{m}/\text{s}^2$ ,  $1/\text{m}$ ], vehicle average speed ( $v$ ) [ $\text{m}/\text{s}$ ], vehicle acceleration ( $a$ ) [ $\text{m}/\text{s}^2$ ] and average slope of the road ( $p$ ). For sake of simplicity, the speed relative to the air will be taken as equal the vehicle average speed whereas the average slope of the road will be assumed as negligible. Finally, the energy consumed by the vehicle along a section is obtained by multiplying the power required to the engine because of the resistance to motion to the time necessary to cross the section:

$$E_{consumed} = P_{electric} \cdot t = \left[ \frac{R_{tot} \cdot v}{\eta_d} + P_{aux} \right] \cdot \frac{L_{section}}{V} \tag{7}$$

Where  $\eta_d$  is the driveline efficiency,  $P_{aux}$  [W] is the auxiliary power, that is the power that includes all consumption not related to the vehicle motion - e.g. lights, air conditioning -,  $L_{section}$  [km] is the length of the road section and  $V$  [km/h] is the vehicle average speed.

The energy received from coils for vehicles in the CWD lane is strictly related to the system element dimensions (EVSE layout and on-board devices), the power provided by coils (PCZ) [kW/m] and the occupancy time of the CZ ( $t_{CZ}$ ), according to the following relationship:

$$E_{received} = P \cdot n_{CZ} \cdot t_{CZ} = (P_{CZ} \cdot LCD \cdot \eta_s) \cdot \left( \frac{L_{section}}{LCZ + I} \right) \cdot \left( \frac{LCZ_{eff}}{V} \right) \tag{8}$$

Where LCD [m] is the on-board device length,  $\eta_s$  is the system efficiency that depends on the distance between the coil(s) of the on-board device and the coil(s) of the CZ installed in the road pavement, LCZ [km] is the length of CZs, I [km] is the inter-distance between CZs and  $LCZ_{eff}$  [km] is the CZ length in which vehicles effectively recharge.  $LCZ_{eff}$  is calculated according to the following relationship:

$$LCZ_{eff} = LCZ - Trk \cdot LCD \tag{9}$$

The coefficient  $Trk$  is introduced to take into account the initial and final partial overlaps between coils on the vehicle and in the pavement that reduce vehicle electric recharges.

#### 4.1.6. SOC update for overtaking

For each section, the ‘‘SOC update for overtaking’’ routine calculates the time in which vehicles cannot recharge because they are overtaking. Vehicle SOC’s at the node are then updated according to the overtaking durations. In the case of a single vehicle overtaking, the time is estimated according to the overtaking model previously described. Instead, if the faster vehicle performs an overtaking maneuver of more than one vehicle, the overtaking time is estimated by taking into account the first and the third lane-changing phases previously described and by calculating the second phase duration as the ratio between the relative distance of the overtaken vehicles and the difference between the average speeds of the fast and the slow vehicles. The scheme of both overtaking maneuver types is reported in Fig. 6.

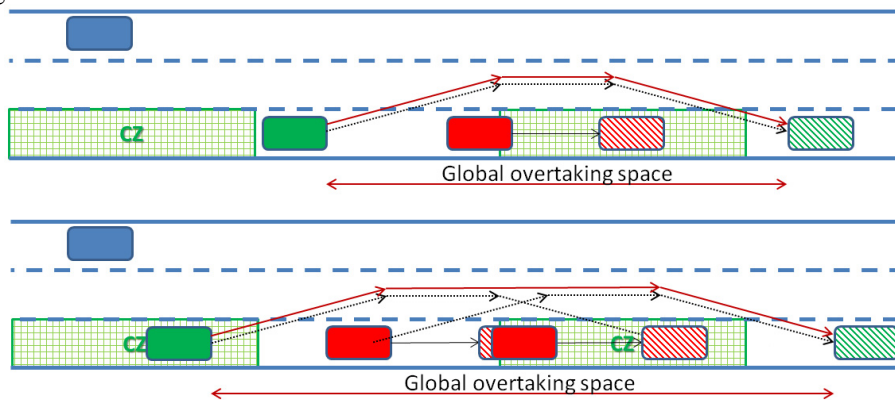


Fig. 6. Schematization of overtaking maneuvers.

4.1.7. Speed test

“Speed test” is a checking routine for traffic conditions next to saturation. It verifies the consistency between vehicle actual average speeds, headways and the minimum spacing that avoids two vehicles overlap. The routine returns an error message if an overlap case is detected. During the experimented simulations this event has never occurred.

4.1.8. Status estimation next

The “Status estimation next” routine returns the lane position (“in” or “out” the CWD lane) and the status (“emer”, “charge”, “no charge”) of each vehicle in the downstream section, according to the updated SOC on the node. By defining its status, the routine assigns to each vehicle its free flow speed, according to recharging speeds set in the CWD lane.

If the strategy is active, during its activation period, the routine excludes that “out” vehicles may enter in the CWD lane at the considered node.

4.1.9. Time estimation next

The “Time estimation next” routine projects vehicles at the following detection point, estimating their arrival times based on free flow speeds related to their status.

If the strategy is active, its effects on traffic are not only limited to the lane closure duration, but extend for a wider period (recovery period). The propagation end time (end queue time) can be estimated according to the scheme reported in Fig. 7.

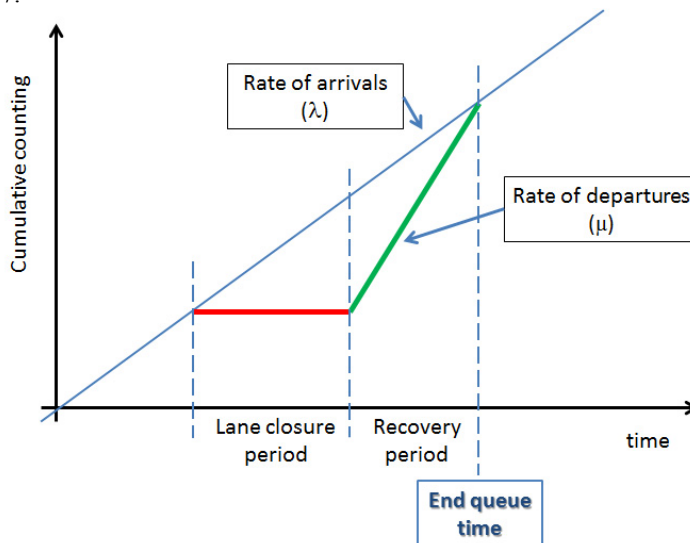


Fig. 7. End queue estimation during the strategy.

The rate of arrivals and departures is estimated based on respectively the number of vehicles arriving on the node and the minimum headway adopted for the vehicle flow before the node involved in the lane closure. For those vehicles whose projected time is included between the initial time of the strategy and the *end queue time*, the routine can operate according to two different approaches. The first one does not perform any further intervention: vehicle relative positions at the *strategy node* are defined according to projections based on two different speed classes. The second approach performs a standardization of vehicle speeds: all vehicles are projected according to the faster speed class. This implies that overtaking maneuvers are not performed along the section approaching the *strategy node*. Long strategy durations lead to very low average speeds in the approaching section. Therefore, overtaking maneuvers would involve very slow vehicles, causing safety problems because of extreme interactions between slow and fast vehicles in “out” lanes. So, the first approach is suggested only for very short time windows. For the

slow vehicle class, the second approach may have another impact: slow vehicles arriving at the *strategy* node shortly after the initial time of the strategy can anticipate the lane closure because their speed is set as the one of the fast vehicle class.

## 5. Verification and validation processes

An extensive verification process has been performed by analyzing, testing and reviewing activities, according to the concepts defined in the ECSS (2009) standards. In particular, a technical verification of the model response is performed based on the following four consecutive test case approach, each one aimed at verifying different aspects:

- *Single vehicle*: this first stage is devoted to ascertain if the single vehicle motion is correctly simulated, as well as the relationship between its behavior and its energy needs. First, a verification of the correspondence between the estimated SOC and the vehicle position, status and speed is performed. Then the verification of the accuracy of the travel time based on the vehicle speeds is assessed. Finally, a verification of the coherence between the implemented energy model and the vehicle SOC trend at each node is conducted.
- *Uniform vehicle flow without overtakes*: this second stage of the consistency verification of the model is developed to assess if the model is able to correctly manage the headways between vehicles, even in the case of new entries.
- *Complex traffic interaction with overtaking maneuvers*: the third stage aims to assess the global interaction between vehicles, introducing overtaking maneuvers. The model has then been tested in a scenario in which overtaking maneuvers are feasible. The number of overtaking maneuvers per section, the identification of the vehicles that are overtaking on the nodes, the time required for the maneuvers and its influence on the SOC trend because of the missed recharge have been verified.
- *Strategy activation*: the last stage checks the consistency of the strategy simulation results in case of incident. A general case of traffic is simulated and vehicle trajectories in the space-time diagram are verified in the neighborhood of the *strategy node*.

At this stage of the CWD development, the presented model has been validated by checking the satisfaction of the established technical requirements, based on the System Engineering approach (INCOSE, 2011). The primary functional requirements used for the validation of the model are the following:

- the model shall estimate the number of vehicles in the CWD lane for any detection point;
- the model shall consider possible random effects of input flows;
- the model shall represent the traffic flow at any detection point and reveal if concentration of traffic and congestion occur along the lane;
- the model shall take into account different values of the minimum headway allowed in the CWD to estimate possible effects on traffic and energy for the various CZs over time;
- the model shall consider also on ramp input flows along the CWD lane to assess possible interactions over time;
- the model shall consider the effects of different scheduling plans on the SOC of the vehicle fleet at the arrival at the depot;
- the model shall involve the possibility of a temporary closure of the CWD lane, without interrupting the service to FEVs.

In the following chapters, the model testing results are reported in an “ideal case”, in which all of the subsystems and applications involved, such as the CWD booking and authorization functions, or the cooperative ADAS, which enables the vehicle cruise control or the cooperative overtaking, work properly. In this scenario, all related system information, such as the vehicle position and its SOC, is accurately known. This validation approach could be considered as a “best-case” testing and it is consistent with the test-case-design methods applied to test software, such as boundary value analysis (Myers et al., 2004), or distributed real time systems (Gutiérrez et al., 1998).

### 6. The CWD scenario and experimental results

The model is applied to the case of a freight distribution service in the city of Turin. After completing their routes, vehicles have to come back to the depot to start a new service in the same day. For this reason, the CWD system is here implemented on the ring road of Turin (Fig. 8), reserving the slower lane to charging activities. The first section in the road model, between nodes 0 and 1, divides the traffic flow between “in” and “out” vehicles and it is not equipped with coils.



Fig. 8. Turin ring road with main secondary accesses.

The considered part of the ring road is characterised by the primary stream and four secondary on ramps, for an overall distance of 18 km. In the road model, all the road sections between nodes have identical lengths, set as 1 km. For each on ramp, an entering traffic flow will be simulated thus increasing the number of vehicles that use the CWD service toward the depot. In detail, all the algorithm input parameters are listed in Table 1 whereas on ramp input flows are reported in Table 2.

Table 1. Inputs to the algorithm.

Type	Input	Value	Unit
Simulation	Number of replications	50	
	Strategy	no/yes	
	Speed control application	yes	
	Strategy node	16	
	Strategy application initial time	1080	s
	Strategy application duration	120	s
Traffic	Average density of the input traffic flow	20	veh/km
	Critical density corresponding to maximum capacity	30	veh/km
	Coefficient of variation of the headway distribution	0.3	
	Maximum traffic headway	1.5	s
Infrastructure	Total length of the road	18	km
	Section length	1	km

	Length of the CZs	20	m
	Inter-distance between CZs	30	m
	System efficiency	0.85	
	Power provided per unit of length	50	kW/m
	Minimum technical headway in CWD lane	2	s
	Speed limit	110	km/h
Vehicle	Average initial SOC	10	kWh
	Standard deviation of the SOC distribution	5	
	Length of the on-board charging device	1	m
	SOC upper threshold for “charge” vehicles	12	kWh
	SOC upper threshold for “emer” vehicles	6	kWh
	Free flow speed for “charge” vehicles	60	km/h
	Free flow speed for “emer” vehicles	30	km/h
	Length	6	m
	Mass	2500	kg
	Cross sectional area	4.9	m <sup>2</sup>
	C <sub>x</sub>	0.38	
	f <sub>0</sub>	0.12	m/s <sup>2</sup>
	f <sub>2</sub>	0.000005	1/m
	Driveline efficiency	0.75	
	Maximum power provided by the engine	60	kW
	Auxiliary power	0.8	kW

Table 2. Input FEVs at each access

Access node	Number of simulated FEVs
0	50
8	50
10	50
13	50
14	50

In particular, this paper describes a traffic model in which FEVs energy requirements have been modeled to take into account the fleet operator need to minimize the recharging time at the depot. At their arrival at the depot, all vehicles must have a minimum SOC level to restart further activities without wasting time for the stationary recharge. In this way, the fleet operator could maintain its level of service, saving the resources needed to install additional structures for vehicle stationary recharges. Deliveries are supposed to be handled by only one type of FEV, a light-van, and the SOC requirement is modeled by taking into account two different classes of speed based on the entrance SOC levels.

Therefore, for a given CWD system and considering one vehicle type, the only parameter that can affect the CWD performance is the vehicle speed. Two operational speed values are implemented, according to previous experiments (Deflorio et al., 2013). The first one allows vehicles to maintain their SOC: it is the speed adopted by vehicles with an adequate level of charge with regards to the SOC requirement of the fleet operator. The range of SOC that satisfies the fleet operator requirement is the one comprised between “charge” and “emer” thresholds. These vehicles are in “charge” status and their speed is set to 60 km/h. The second speed (30 km/h) guarantees a proper recharge - 1 kWh after about 2.7 km - and it is adopted by vehicles in “emer” status, whose SOC is low and minor than the “emer” threshold”.

The CWD system model has been tested in several traffic scenarios to reveal its capability in simulating relevant effects interesting for CWD operations. The traffic along the CWD lane depends also from the demand structure and therefore from the input flows entering at the various on ramps of the ring road. For this reason, we have assumed two reference scheduling plans of the freight distribution service, according to different possible fleet management strategies.

The first one refers to the case where all vehicles distributing or picking parcels in the various zones of the city center complete their services almost contemporary. In this case, interactions along the ring road will be less relevant and arrivals to the depot will be distributed over a wider time period because vehicles start to enter into the ring road almost simultaneously, but in different nodes. Following this strategy, vehicle delivery missions should have almost identical durations for the various zones of the city.

In the second scenario, the service management strategy is oriented to concentrate all return trips in a smaller time window. In this case, vehicles coming from farther zones will enter into the ring road earlier than closer vehicles. Adopting this strategy, vehicle delivery missions are on average longer for the closer zones of the city, because FEVs can come back to the depot in a shorter time.

As usual in traffic analyses, results depend on many random factors affecting the model rules at different levels. In the simulated cases, the focus on random phenomena is related to the features of input flows at various entries.

### 6.1. Scenario 1 - Simultaneous end of service in the city center

The scenario variability is illustrated by Fig. 9 in which the number of vehicles (# veh) using the CWD for the whole simulation period, detected node by node is reported for 50 replications.

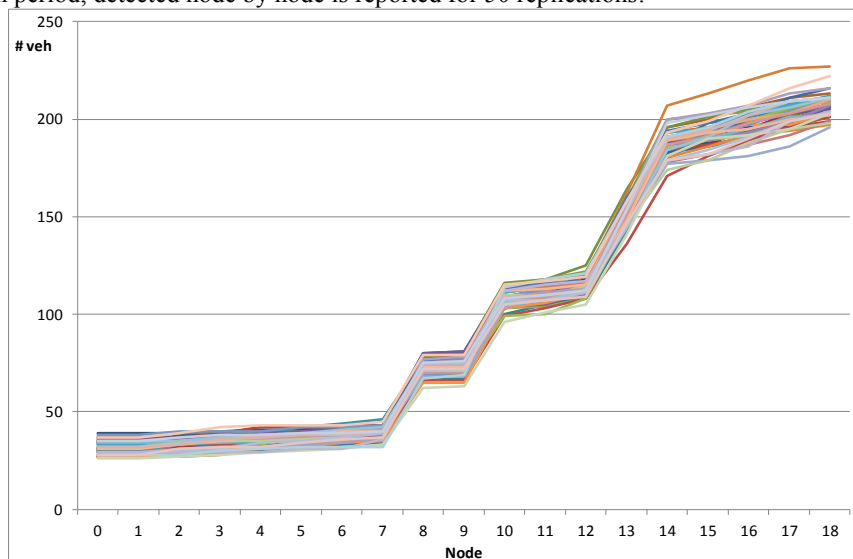


Fig. 9. Variability of the traffic flows in the CWD lane for 50 replications for scenario 1.

The following analysis will focus on one sample replication to better check traffic and energy behaviors in the implemented simulation model. The replication #16 is selected for its significance because, with respect to the indicator “# veh”, it is in the range [mean-std, mean+std] for all the nodes as represented in Fig. 10.

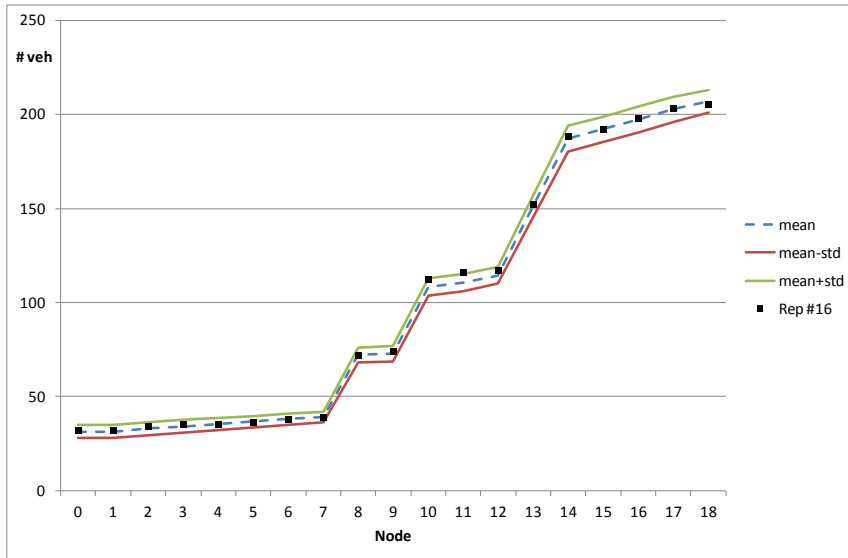


Fig. 10. Sample replication with respect to the replication distribution of Scenario 1.

The first result analyzed of the selected replication is the chart illustrating space-time relationship for all vehicles using the CWD service, node by node (Fig. 11). This chart describes the use of the various zones of the CWD system during the period of analysis. Different slopes refer to different speed classes for “emer” and “charge” vehicles and slope reductions represent speed variations when “emer” vehicles become “charge”. As expected, the most part of the interactions takes place in the final part of the ring road, during the time window between 300s and 1200s.

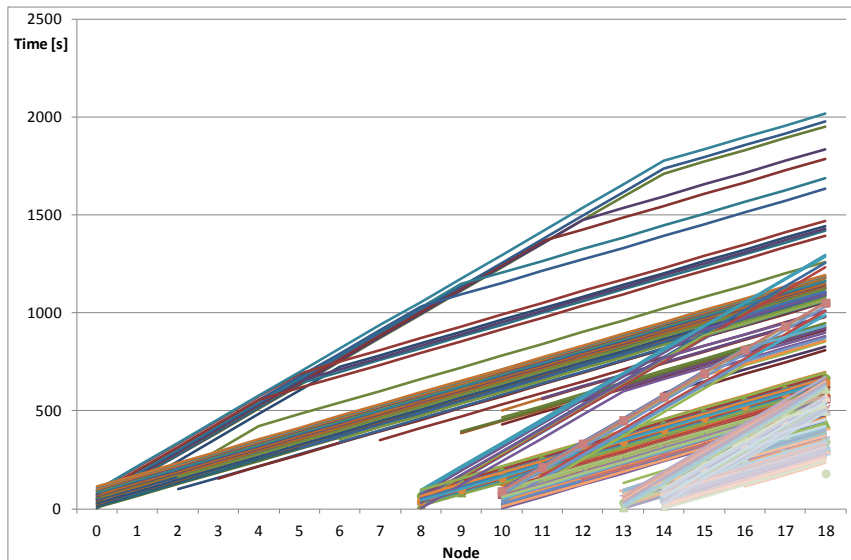


Fig. 11. Space-time relationship for “in” vehicles in scenario 1.

To provide a more “traffic oriented” idea on simulation results, the counting and average speeds of the vehicles in the CWD lane have been reported in the following charts (Fig. 12 and Fig. 13) for a time resolution of 1 minute at



each node of the ring road modeled. The average speed data refers only to “charge” vehicles because the speed of “emer” vehicles is always 30 km/h and it is not relevant to show.

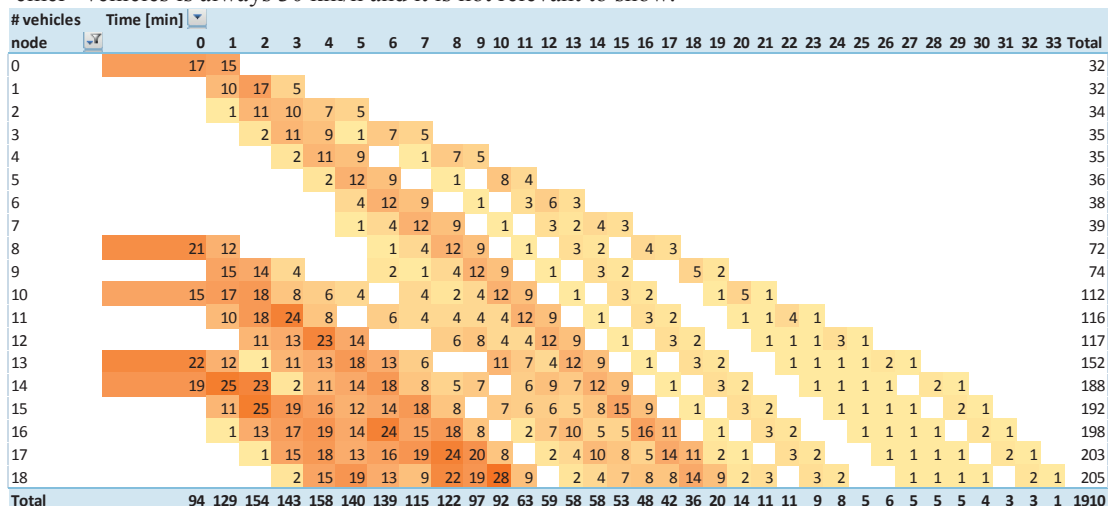


Fig. 12. Count of “in” vehicles, node by node, with a 1 min time resolution in scenario 1.

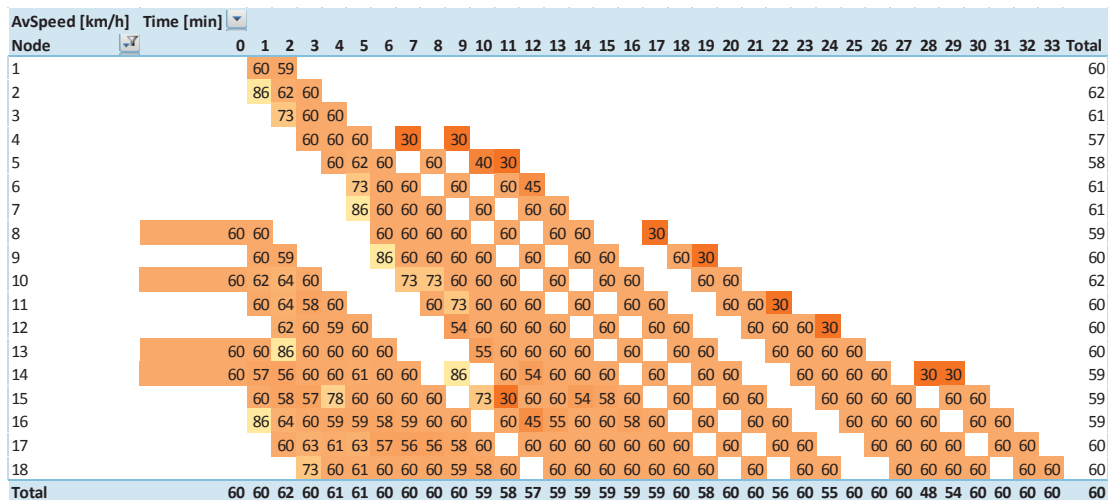


Fig. 13. Average speeds [km/h] of "in" and "charge" vehicles, node by node, with a 1 min time resolution in scenario 1.

The two charts show where and when relevant congestion events are detected by the model - contemporary high counting values and low average speeds -. In this scenario, only few slowdowns occur and they are quite limited and observable only in the final part of the ring road - after the node 12 -.

6.2. Scenario2 - Simultaneous arrival at depot

This scenario represents a planning case where the delivery plan has been set with a balanced use of vehicles for the whole morning period, with almost the identical trip duration for all vehicles. This plan requires shorter delivery durations for farther zones than for closer ones. According to the approach of scenario 1, the variability of scenario 2 is represented by the number of vehicles in the CWD lane for the whole simulation period, detected for 50 replications node by node. The trend, reported in Fig. 14, is quite similar of that one in Fig. 9, considering that the

total number of simulated vehicles is identical and the only difference is related to the time when vehicles entry in the CWD lane.

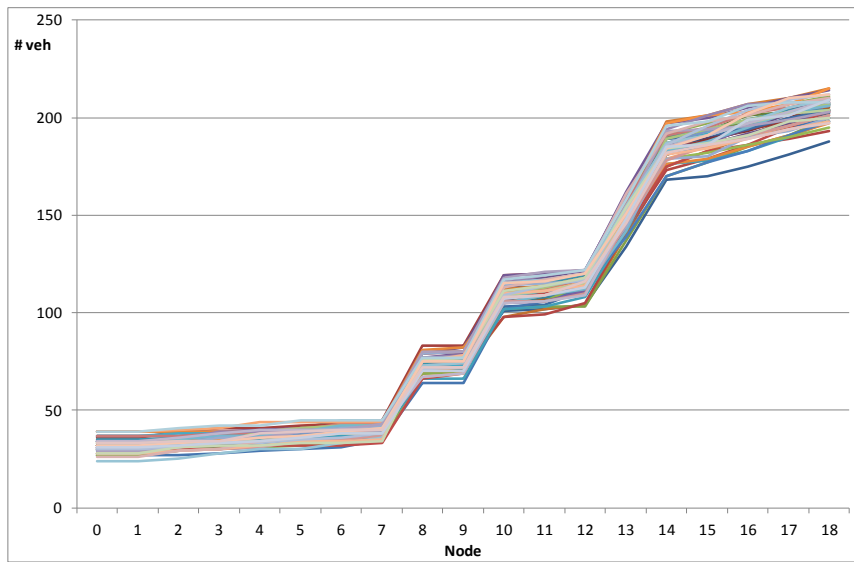


Fig. 14. Variability of the traffic flows in the CWD lane for 50 replications for scenario 2.

The replication selected for its significance is the #2, because it is in the range [mean-std, mean+std] for all the nodes, as depicted in Fig. 15.

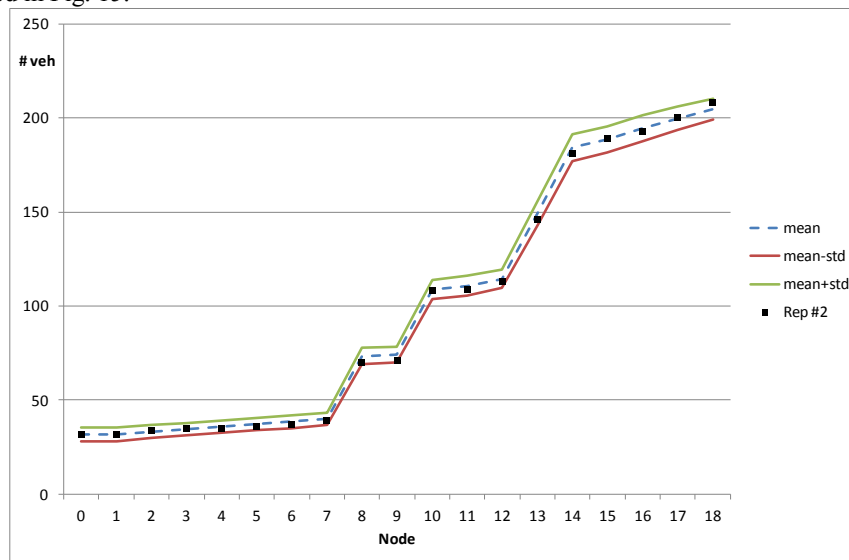


Fig. 15. Sample replication with respect to the replications distribution of Scenario 2.

The identifying characteristic of this scenario is clearly illustrated in Fig. 16: flows entering from the intermediate on ramps use the CWD lane when the mainstream flow arrives at the considered access nodes. The effect of the vehicle concentration in a smaller time period is evident in Fig. 17 reporting vehicle counting for each node for a time interval of 1 minute.

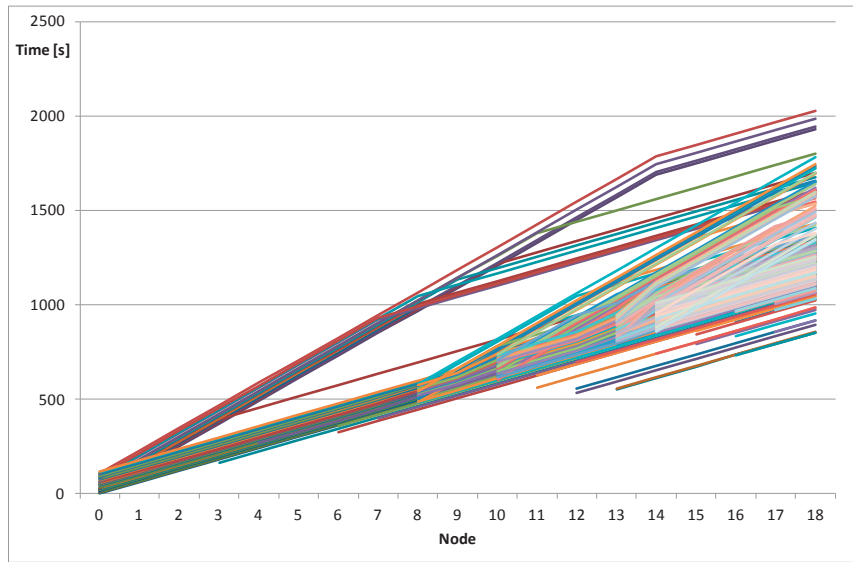


Fig. 16. Space-time relationship for "in" vehicles in scenario 2.

Count Nv	time [min]																																		Total				
Node	0	1	2	3	4	5	6	7	8	9	10	11	12	13	14	15	16	17	18	19	20	21	22	23	24	25	26	27	28	29	30	31	32	33	Total				
0	19	13																																	32				
1		12	18	2																																32			
2			14	11	7	2																															34		
3				1	14	11		7	2																												35		
4					1	14	11		1	6	2																										35		
5						1	14	11		1		6	2																								36		
6							2	1	14	11		1		1	5	2																					37		
7								2	3	14	11		1		1	6	1																				39		
8									1	2	3	29	26		1		1	5	1																		70		
9										1	3	3	26	26	3	1		1		1	1	4	1														71		
10											1	4	4	30	30	27	4		1		1	1		4	1												108		
11												2	4	4	25	30	26	7	3	1		1	1		4	1											109		
12													1	2	4	6	26	25	28	4	7	3		1	1		4	1									113		
13														1	2	5	8	28	30	30	22	5	7	1	1	1		2	2	1							146		
14															1	3	6	10	29	30	30	30	24	5	5	2	1											181	
15																3	3	8	11	26	27	29	30	24	12	4	5	2										189	
16																	3	3	8	12	27	24	26	30	28	6	11	4	5	1								193	
17																		3	3	8	16	29	25	22	27	28	9	6	10	5	3	1						200	
18																			3	5	11	18	29	26	22	23	25	10	9	4	11	3	3	1	2				208
<b>Total</b>	<b>19</b>	<b>25</b>	<b>33</b>	<b>29</b>	<b>35</b>	<b>31</b>	<b>38</b>	<b>35</b>	<b>57</b>	<b>66</b>	<b>74</b>	<b>79</b>	<b>110</b>	<b>110</b>	<b>126</b>	<b>121</b>	<b>147</b>	<b>141</b>	<b>147</b>	<b>111</b>	<b>100</b>	<b>65</b>	<b>55</b>	<b>23</b>	<b>28</b>	<b>13</b>	<b>18</b>	<b>7</b>	<b>7</b>	<b>6</b>	<b>5</b>	<b>3</b>	<b>3</b>	<b>1</b>	<b>1868</b>				

Fig. 17. Count of "in" vehicles, node by node, with a 1 min time resolution in scenario 2.

The effect on congestion is confirmed by average speeds, reported in Fig. 18 for the "charge" vehicle class. The lower values – even lower than 40 km/h - are detected at nodes 13 and 14 in the time interval [13,18]. Values of 30 km/h refer to vehicles that change their status from "emer" to "charge" and not to traffic interactions.

AvSpeed [km/h]	time [min]																																	Total	
Node	1	2	3	4	5	6	7	8	9	10	11	12	13	14	15	16	17	18	19	20	21	22	23	24	25	26	27	28	29	30	31	32	33	Total	
1	60	59																																60	
2		64	60																															62	
3			86	60	60																													60	
4				60	60	60																												60	
5					86	60	60	60																										60	
6						73	60	60	60																									60	
7							60	78	60	60																								62	
8								86	60	60	57	55																						57	
9									60	69	60	60	59																					60	
10										60	66	67	55	42	36	60																		48	
11											73	60	60	60	58	57	60	30	60															59	
12												86	60	60	69	61	60	58	59	45	45													59	
13													60	60	64	66	57	49	40	36	60	60												50	
14														60	69	64	65	56	49	41	34	35	60	30	60	60	60							47	
15															78	60	66	62	62	58	57	54	51	60	60	60	60							58	
16																60	60	60	62	61	61	58	57	57	60	45	60	45							59
17																	60	60	60	67	61	59	60	59	57	50	50	60	60						60
18																		60	71	66	63	59	59	60	60	59	48	60	45	60					60
Total	60	63	61	61	61	61	61	60	59	57	55	55	59	56	54	54	55	57	58	59	57	51	49	55	60	45	60	45	50	60	60	60	60	57	

Fig. 18. Average speeds [km/h] of "in" and "charge" vehicles, node by node, with a 1 min time resolution in scenario 2.

In this scenario, the congestion effect involves also "emer" vehicles, as shown in Fig. 19: at node 14, during the minute 17, their speed decreases to 22 km/h.

AvSpeed [km/h]	time [min]																												Total
Node	2	3	4	5	6	7	8	9	10	11	12	13	14	15	16	17	18	19	20	21	22	23	24	25	26	27	28	Total	
1	30	30																										30	
2		30	30																									30	
3			30	30																								30	
4				30	30																							30	
5					30	30																						30	
6						30	30																					30	
7							30	30																				30	
8								30	30																			30	
9									29	30																		30	
10										30	30																	30	
11											29	30																30	
12												30	30															30	
13													30	30	30													30	
14														30	29	24	22	24	30	30	30							27	
15															29	29	28	28	30	30	30	30						29	
16																30	29	29	30	30	30	30	30					30	
17																	30	29	30	30	30	30	30	30				30	
18																			29	30	30	30	30	30	30	30		30	
Total	30	30	30	30	30	30	30	30	30	29	30	30	30	28	28	28	29	30	30	30	30	30	30	30	30	30	30	29	

Fig. 19. Average speeds [km/h] of "in" and "emer" vehicles, node by node, with a 1 min time resolution in scenario 2.

6.3. Comparison of energy and traffic performance in the two scenarios

To show the possible differences between the two scenarios also from the energy point of view, the average SOC of the entire fleet is monitored node by node every minute. This analysis is not focused on a single replication but it is averaged on 50 replications to obtain a more stable result.

Average SoC [kWh]	Time [min]																																		Total																	
Node	0	1	2	3	4	5	6	7	8	9	10	11	12	13	14	15	16	17	18	19	20	21	22	23	24	25	26	27	28	29	30	31	32	33	Total																	
0		7.1	7.2	9.0																															7.1																	
1			8.8	6.8	3.5																															6.9																
2				11.4	9.0	8.9	3.9	3.8																												7.2																
3					11.4	9.2	8.9	6.4	4.2	4.2																										7.5																
4						11.5	11.4	9.3	9.0	6.7	6.5	4.5	4.5																							7.8																
5							11.4	11.4	9.4	9.0	6.7	6.6	6.6	4.9	4.6																					8.0																
6								11.4	11.4	9.4	9.1	6.7	6.6	6.6	6.6	5.0	4.8																			8.2																
7									11.4	11.4	11.4	9.4	9.1	6.7	6.6	6.6	6.6	5.1	4.9																	8.4																
8										7.0	7.2																									7.9																
9											9.2	6.6	3.5																							8.0																
10												7.1	7.1	9.4	9.2	3.7	3.9	11.4	11.4	11.4	11.5	9.4	9.1	6.8	6.6	6.6	6.6	6.6	6.6	6.6	5.7	5.5				7.9																
11													9.2	7.1	7.9	9.2	6.6	4.0	4.3	11.4	11.4	11.5	9.4	9.1	6.8	6.6	6.6	6.6	6.6	6.6	5.9	5.8				8.1																
12														11.4	9.3	9.4	7.8	7.4	6.6	6.5	4.4	6.9	11.5	11.5	9.4	9.1	6.8	6.6	6.7	6.6	6.6	6.6	6.1	6.0		8.3																
13															7.0	6.9	11.4	9.5	9.6	9.4	7.3	4.3	6.5	9.3	6.4	8.3	11.5	9.5	9.1	6.8	6.7	6.7	6.6	6.6	6.6	6.3	6.3	8.1														
14																7.0	7.9	6.6	5.7	9.6	9.6	9.5	9.0	4.3	4.9	9.8	10.2	7.5	8.4	9.5	9.1	6.8	6.7	6.7	6.6	6.6	6.6	6.5	6.6	6.6	8.0											
15																		9.1	7.9	7.3	5.9	8.4	9.7	9.5	9.0	6.6	5.1	6.6	10.2	10.6	7.6	8.6	9.2	6.8	6.7	6.7	6.7	6.6	6.6	6.6	6.6	6.6	6.6	8.2								
16																			11.4	9.4	9.3	7.5	6.7	8.1	8.2	9.5	9.0	6.6	7.8	6.5	7.5	10.6	10.7	8.3	8.3	6.8	6.7	6.7	6.7	6.6	6.6	6.6	6.6	6.6	6.6	8.3						
17																					11.4	9.6	9.4	9.4	7.2	8.4	8.1	8.2	9.0	6.7	8.1	9.4	7.3	8.3	10.7	9.3	8.0	4.8	6.7	6.7	6.7	6.7	6.6	6.6	6.6	6.6	6.6	6.6	8.5			
18																						11.4	11.4	9.7	9.4	9.5	10.3	8.5	8.2	8.1	7.7	7.1	8.4	9.4	9.5	8.1	8.5	9.3	9.1	4.8	5.1	6.7	6.7	6.7	6.7	6.6	6.6	6.6	6.6	6.6	6.6	8.6
Total		7.0	8.1	8.0	8.5	8.4	8.6	8.4	8.5	8.3	8.3	8.3	8.2	8.2	8.2	8.5	8.3	8.5	8.2	8.2	8.0	7.4	5.9	6.0	6.4	6.4	6.5	6.4	6.5	6.5	6.6	6.6	6.6	6.6	6.6	6.6	6.6	6.6	6.6	6.6	6.6	6.6	6.6	6.6	6.6	6.6	6.6	6.6	8.1			

Fig. 20. Average SOC [kWh] of "in" vehicles, node by node, with a 1 min time resolution, for scenario 1.

Average SoC [kWh]	Time [min]																																		Total																			
Node	0	1	2	3	4	5	6	7	8	9	10	11	12	13	14	15	16	17	18	19	20	21	22	23	24	25	26	27	28	29	30	31	32	33	Total																			
0		7.1	6.9																																			7.0																
1			8.8	6.7	3.4																																	6.8																
2				11.4	9.0	8.8	3.9	3.7																														7.1																
3					11.4	9.3	8.8	6.2	4.2	4.1																												7.5																
4						11.4	11.4	9.4	9.0	6.6	6.5	4.6	4.4																									7.7																
5							11.4	11.4	9.4	9.0	6.6	6.6	6.6	4.8	4.5																							8.0																
6								11.4	11.4	9.4	9.0	6.6	6.6	6.6	6.6	4.9	4.7																					8.2																
7									11.3	11.4	11.4	9.4	9.0	6.6	6.6	6.6	6.6	6.6	5.0	4.9																		8.4																
8										11.4	11.4	11.4	7.9	7.8	7.0	6.6	6.6	6.6	6.6	6.6	5.2	5.2																7.8																
9											11.4	11.4	11.5	9.3	7.9	4.1	6.0	6.6	6.6	6.6	6.6	6.6	5.4	5.3														8.0																
10												11.4	11.4	11.4	11.5	8.3	8.3	7.5	4.1	6.2	6.6	6.6	6.6	6.6	5.7	5.5											7.9																	
11													11.4	11.4	11.5	9.4	8.5	7.9	4.4	4.2	6.2	6.6	6.6	6.6	6.6	5.8	5.8										8.1																	
12														11.4	11.4	11.4	11.5	9.5	9.4	8.1	4.9	4.5	4.4	6.2	6.6	6.6	6.6	6.6	6.5	6.1	6.0							8.3																
13															11.4	11.4	11.4	11.5	8.9	8.4	8.6	7.9	4.7	4.6	4.6	6.2	6.6	6.6	6.6	6.6	6.6	6.3	6.3					8.2																
14																11.4	11.4	11.4	11.5	8.7	8.5	8.4	8.9	7.3	4.9	4.7	4.6	6.2	6.6	6.6	6.6	6.6	6.6	6.6	6.6	6.6	6.6	6.6	6.6	6.6	6.6	6.6	6.6	6.6	6.6	6.6	6.6	6.6	8.3					
15																		11.4	11.4	11.4	11.5	11.5	9.6	8.9	8.6	8.7	7.9	4.8	5.0	4.8	4.6	6.2	6.6	6.6	6.6	6.6	6.6	6.6	6.6	6.6	6.6	6.6	6.6	6.6	6.6	6.6	6.6	6.6	6.6	6.6	8.4			
16																				11.4	11.4	11.4	11.5	11.5	9.7	9.6	8.9	8.9	7.9	5.5	4.8	5.1	4.9	4.7	6.3	6.6	6.6	6.6	6.6	6.6	6.6	6.6	6.6	6.6	6.6	6.6	6.6	6.6	6.6	6.6	6.6	8.6		
17																						11.5	11.4	11.4	11.4	11.5	11.5	9.8	9.6	9.5	9.2	8.2	5.5	5.2	4.9	5.2	4.9	4.9	6.2	6.6	6.6	6.6	6.6	6.6	6.6	6.6	6.6	6.6	6.6	6.6	6.6	6.6	8.7	
18																							11.4	11.4	11.4	11.5	11.5	11.5	9.9	9.9	9.7	9.5	9.7	8.5	5.9	5.1	5.2	5.0	5.2	5.0	4.9	4.9	6.3	6.6	6.6	6.6	6.6	6.6	6.6	6.6	6.6	6.6	6.6	8.9
Total		7.1	7.8	7.8	8.2	8.4	8.6	8.8	8.9	8.9	8.3	8.6	8.4	8.6	8.8	8.8	8.6	8.7	8.8	8.9	8.6	8.5	8.0	7.7	6.7	5.5	5.2	5.4	5.4	5.5	5.8	5.9	6.6	6.6	6.6	6.6	6.6	6.6	6.6	6.6	6.6	6.6	6.6	6.6	6.6	6.6	6.6	6.6	6.6	8.3				

Fig. 21. Average SOC [kWh] of "in" vehicles, node by node, with a 1 min time resolution, for scenario 2.

Although in scenario 2 the final SOC of the fleet at depot - node 18 - is higher on average with respect to scenario 1 - 8.9 kWh instead of 8.6 kWh -, a detailed analysis reveals that in scenario 2 more cases of vehicles with low SOC occur from minute 22 to minute 29. Indeed in Scenario 1 only in minutes 19 and 20 vehicles arrive with an average SOC less than 6 kWh. Different fleet SOC at the depot can be managed by the distribution service planner by assigning a proper task and maybe related route to various vehicles according to their SOC.

Concerning the average delay, calculated as the difference between the “free flow” conditions and the estimated travel time, scenario 1 has very few delays, mostly in the final part of the CWD lane and in the first part of the simulated period (Fig. 22). On the contrary, scenario 2 presents higher delays and they occur in the identical part of the CWD lane but in the middle of the simulation period (Fig. 23).

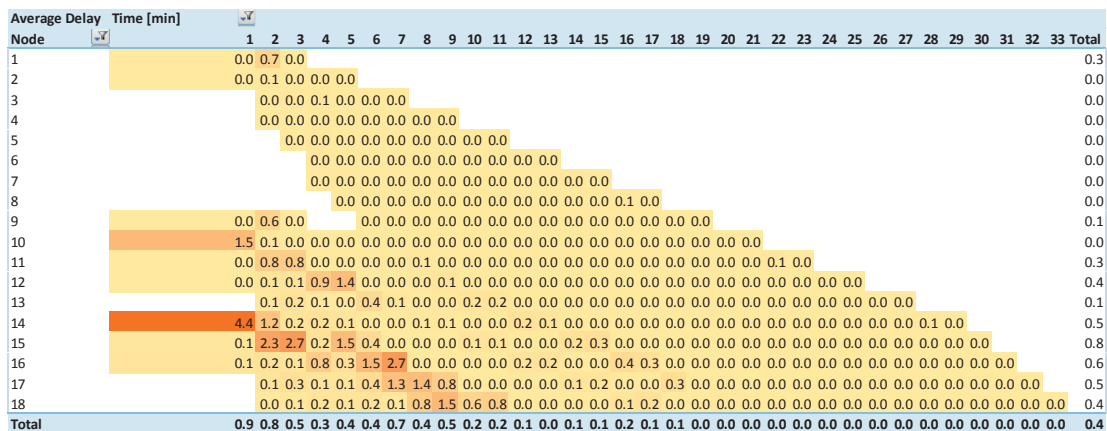


Fig. 22. Delays [s] of "in" vehicles, node by node, with a 1 min time resolution, for scenario 1.

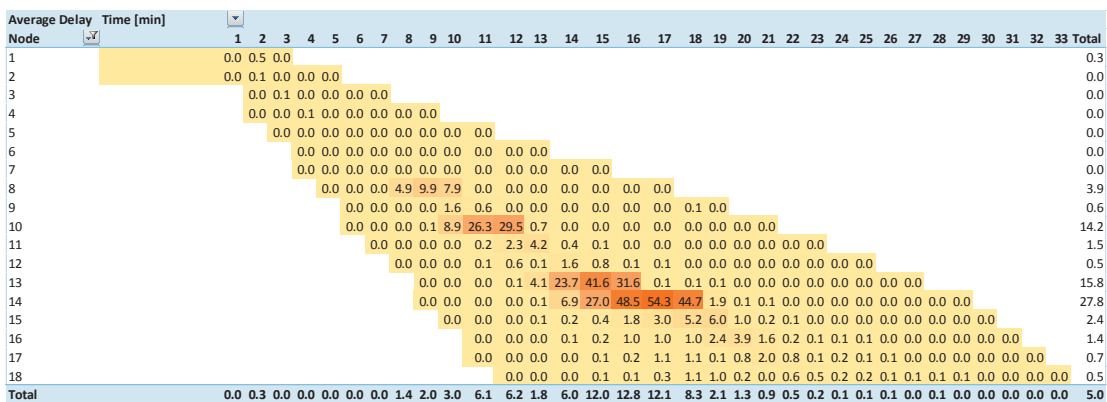


Fig. 23. Delays [s] of "in" vehicles, node by node, with a 1 min time resolution, for scenario 2.

In a congested scenario, as scenario 2, the average charging time should increase because of the lower average speeds. However, overtaking maneuvers are relevant in congested cases and vehicles do not recharge during the maneuver. To verify this consideration, the average number of overtaking maneuvers is detected and reported in Fig. 24 for scenario 1 and in Fig. 25 for scenario 2.

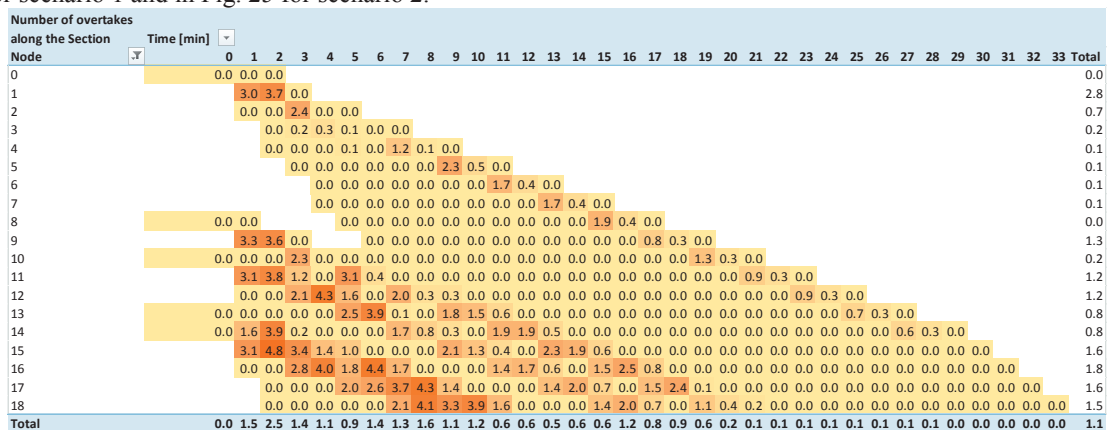


Fig. 24. Number of overtaking maneuvers detected in the CWD lane, node by node, with a 1 min time resolution, for scenario 1.

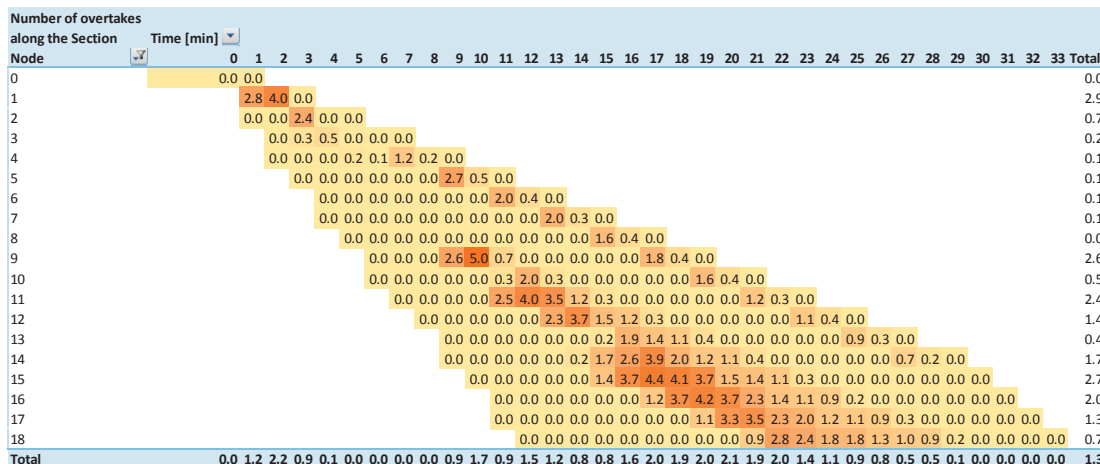


Fig. 25. Number of overtaking maneuvers detected in the CWD lane, node by node, with a 1 min time resolution, for scenario 2.

In scenario 2 a higher number of overtakes concentrated after the node 14 and during the time interval [15, 25] confirms the previous considerations. In scenario 1 the overtaking maneuvers are relevant in those sections, but in another time interval [1, 10] and therefore they do not affect the mainstream flow.

#### 6.4. Scenario 3: Simultaneous arrival with a CWD lane service interruption

The conditions of Scenario 2, which is the critical one, can also be monitored in the case of an incident involving the CWD lane. For various reasons, such as maintenance, cleaning or inspection of the coils, the CWD lane could be out of service in a particular node and it should be kept free of traffic for a certain period. This vehicle-free time window can be obtained by reducing vehicle speeds in the CWD lane along the section approaching the node involved in the incident - modeled by "Headway correction" and "Time estimation next" routines -. The strategy will be applied by avoiding overtaking maneuvers in the approaching section.

In the experiments performed, the CWD lane closure lasts two minutes, starting from the 18th minute- 1080s from the beginning of the simulation -. The data reported is averaged on 50 replications to show more reliable results.

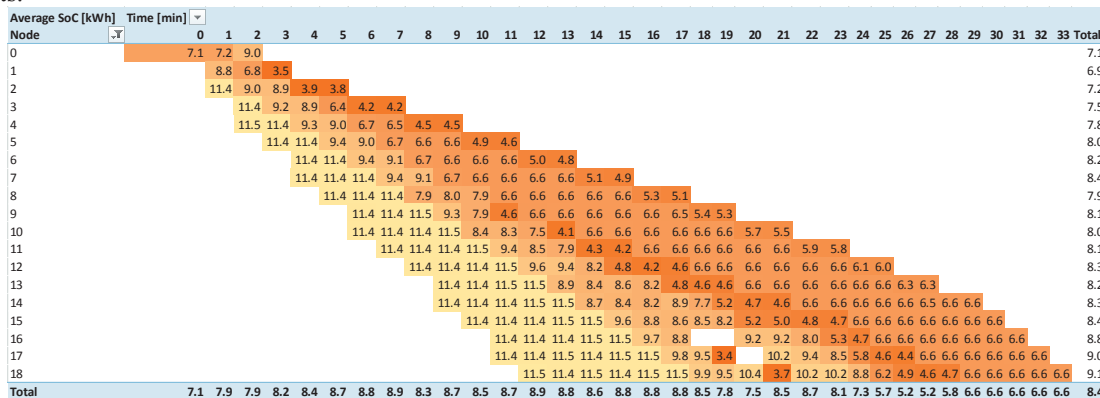


Fig. 26. Average SOC [kWh] of "in" vehicles, node by node, with a 1 min time resolution, for scenario 3.

The impact of the incident on the SOC is shown in Fig. 26 in which the missing data for minutes 18 ad 19 confirm the CWD lane closure for that period at node 16. Data also show that vehicles arriving at the depot after the temporary closure have a higher SOC than those in scenario 2 (see Fig. 21). The lower SOC values – 3.4 and 3.7

kWh – refers to “emer” vehicles that have avoided the lane closure because of the speed regulation. Indeed, their charging time has been reduced because their speed has been set to 60 km/h. The propagation of the strategy effects can be analyzed by average speeds. The average speed reductions, as a result of the simulation, are confirmed in Fig. 27 for the section approaching the node 16 during the time interval [20,23], in which the average speed drops off even to 20 km/h at minute 20.

AvSpeed [km/h]	Time [min]																																		Total			
Node		1	2	3	4	5	6	7	8	9	10	11	12	13	14	15	16	17	18	19	20	21	22	23	24	25	26	27	28	29	30	31	32	33	Total			
1		60	48	30																																		49
2		86	62	61	30	30																															51	
3		74	61	59	32	30	30																													50		
4		86	69	61	60	32	44	31	30																											51		
5		79	66	60	60	60	60	60	32	30																									53			
6		74	67	60	60	60	60	60	60	33	30																							54				
7		86	69	63	60	60	60	60	60	60	33	30																					55					
8		79	66	61	52	51	52	60	60	60	60	33	30																			51						
9		74	64	60	60	52	36	58	60	60	60	60	32	30																	53							
10		86	72	63	63	52	46	38	33	58	60	60	60	32	30															46								
11		80	69	62	64	60	54	50	34	33	59	60	60	60	34	30													52									
12		75	66	61	66	61	60	53	38	34	36	59	60	60	60	34	30											54										
13		75	63	63	65	54	45	40	35	37	36	36	60	60	60	60	34	30									46											
14		86	69	62	64	63	53	45	37	30	30	38	37	36	60	60	60	60	34	30							42											
15		78	66	61	65	63	61	55	53	50	48	40	40	36	37	60	60	60	60	60	60					53												
16		72	63	62	64	63	61	59		20	21	23	39	60	60	60	60	60	60	60	60					41												
17		86	68	62	65	64	63	60	59	30	60	54	51	45	34	36	60	60	60	60	60					55												
18		83	67	61	65	62	62	60	60	59	30	60	60	55	49	38	32	36	60	60	60					56												
Total		61	55	56	55	56	56	56	53	55	53	52	53	55	51	50	49	50	49	49	29	39	44	50	51	44	40	38	43	52	60	60	60	60	50			

Fig. 27. Average speeds [km/h] of "in" and "emer" vehicles, node by node, with a 1 min time resolution, for scenario 3.

The speed reduction has a sensible effect on the delay of the vehicles, estimated as the difference between the simulated travel time and the predicted travel time on the base of the planned speed. As expected, the higher delays occur in the section before the node 16, during the *recovery period*. Also negative values of delay are detected: they are caused by the speed change for “emer” vehicles that are forced to proceed at the speed of the “charge” vehicles during the “safety” control action. This case is represented in Fig. 29 in which the trajectories of all the charging vehicles are traced for a sample replication (#2). The trajectory of the vehicle #237, represented by black dots, shows that, if it travelled at 30 km/h, it would have been involved in the lane closure at node 16. However, because of the speed control action, it increases its speed and it crosses the node 16 before the incident event. After the node 16, its speed is set again at 30 km/h, as required by its charging needs, and it is then maintained until the final node.

AvDelay [s]	Time [min]																																		Total			
Node		1	2	3	4	5	6	7	8	9	10	11	12	13	14	15	16	17	18	19	20	21	22	23	24	25	26	27	28	29	30	31	32	33	Total			
1		0.0	0.7	0.0																																		0.3
2		0.0	0.1	0.0	0.0	0.0																															0.0	
3		0.0	0.0	0.1	0.0	0.0	0.0																													0.0		
4		0.0	0.0	0.0	0.0	0.0	0.0	0.0																											0.0			
5		0.0	0.0	0.0	0.0	0.0	0.0	0.0	0.0																									0.0				
6		0.0	0.0	0.0	0.0	0.0	0.0	0.0	0.0	0.0																							0.0					
7		0.0	0.0	0.0	0.0	0.0	0.0	0.0	0.0	0.0	0.0																					0.0						
8		0.0	0.0	0.0	1.3	3.4	8.9	0.0	0.0	0.0	0.0	0.1	0.0																			1.8						
9		0.0	0.0	0.0	0.0	2.1	1.5	0.0	0.0	0.0	0.0	0.0	0.0	0.0																	0.9							
10		0.0	0.0	0.0	0.0	3.6	13.2	23.6	0.6	0.0	0.0	0.0	0.0	0.0	0.0	0.0															9.8							
11		0.0	0.1	0.0	0.0	0.3	2.0	4.1	0.4	0.0	0.0	0.0	0.0	0.0	0.0	0.0	0.1	0.0													1.4							
12		0.0	0.0	0.0	0.1	0.7	0.2	1.2	0.2	0.1	0.1	0.0	0.0	0.0	0.0	0.0	0.0	0.0	0.0	0.0											0.5							
13		0.0	0.0	0.1	0.2	3.2	14.0	26.8	37.7	1.4	0.1	0.1	0.0	0.0	0.0	0.0	0.0	0.0	0.0	0.0									13.8									
14		0.0	0.0	0.0	0.1	0.1	3.8	15.0	33.6	55.6	50.1	8.1	0.1	0.0	0.0	0.0	0.0	0.0	0.0	0.1	0.0							24.0										
15		0.0	0.0	0.0	0.1	0.2	0.3	1.8	2.7	5.5	7.4	1.7	0.1	0.1	0.1	0.0	0.0	0.0	0.0	0.0	0.0					2.6												
16		0.1	0.0	0.0	0.2	0.2	0.8	-6.0		106.2	102.6	88.4	9.3	-40.0	0.0	0.0	0.0	0.0	0.0	0.0					44.2													
17		0.0	0.1	0.0	0.1	0.1	0.2	1.0	0.6	0.0		0.0	1.6	4.2	1.7	0.2	0.0	0.0	0.0	0.0	0.0					1.2												
18		0.0	0.0	0.0	0.0	0.1	0.2	0.7	0.3	1.0	0.0	0.1	0.0	1.1	1.5	0.2	0.1	0.0	0.0	0.0	0.0					0.4												
Total		0.0	0.4	0.0	0.0	0.0	0.0	0.7	1.3	2.2	4.9	6.0	1.8	4.7	9.7	12.9	10.9	11.4	3.5	60.3	41.8	28.2	3.5	-2.1	0.8	0.1	0.1	0.0	0.0	0.0	0.0	0.0	0.0	9.4				

Fig. 28. Delays [s] of "in" vehicles, node by node, with a 1 min time resolution, for scenario 3.



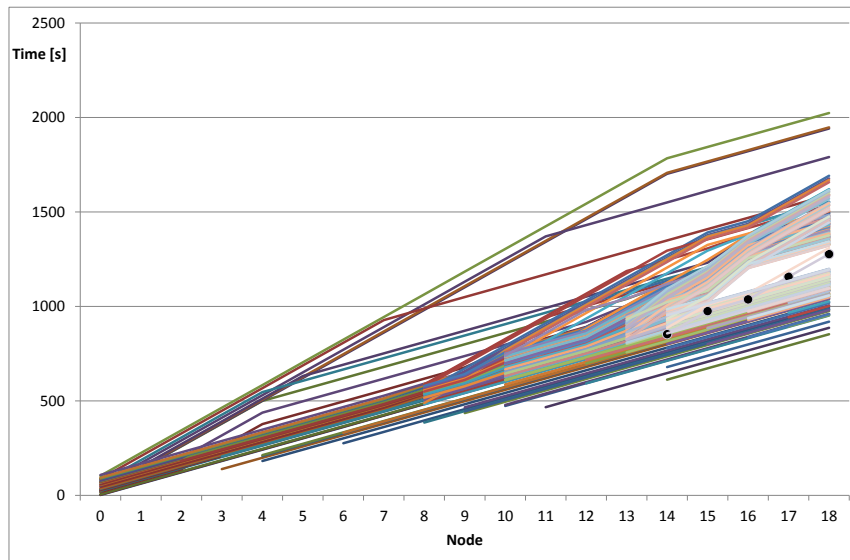


Fig. 29. Space-time relationship for "in" vehicles in the case of application of the strategy.

## 7. Conclusions and further researches

This study presents a method for assessing the performance of the wireless power systems to dynamically charge electric vehicles while driving, from both traffic and energy points of view. The model assumptions are aimed at simulating a freight scenario for urban distribution in the city center with medium sized vans. The CWD lane has been modeled in a realistic layout, as installed on a ring road with secondary on ramps, for supporting electric charging operations during the return part of the vehicle trips. The set of speeds for CWD operations is relatively low because, for the assumed  $P_{cz}$  and the test vehicle considered, it is the most adequate to satisfy the fleet operator need to guarantee a minimum SOC at the vehicle arrivals to the depot.

The implemented dynamic traffic simulator adopts a mesoscopic approach by updating traffic and energy data only at defined nodes along the road, generally spaced in the order of hundreds of meters. The traffic simulator operates according to a cooperative driving behavior among vehicles, both for the overtaking maneuvers and the entries management and it is able to simulate different traffic conditions. Primary traffic parameters can be estimated in the CWD lane, such as the vehicle counting, average speeds and delays, which are time dependent and relevantly change along the road. The model also allows the implementation of a speed control strategy to manage temporary incidents, for example due to extraordinary maintenance operations. This strategy could also be applied in the case of high traffic volumes to facilitate the entries of the vehicles from the on ramps. The traffic model is able to manage even platooning conditions and delays caused by the strategy when minimum headways in the CWD lane are required and it is able to assess the effects of the strategy in terms of vehicle SOCs and speeds over time. With respect to the traditional dynamic traffic models, in the proposal here presented, the current vehicle energy needs affect drivers' behavior. According to their SOC along the road, vehicles are simulated inside or outside the charging lane and their speeds are set according to their charging needs.

The implemented dynamic traffic simulator has an approximation compatible with the stage of development of the CWD technology and the deployment of the cooperative driving systems. For this reason, in our idea, the presented model should be considered as a support methodology of a feasibility study for a promising future technology, in ex-ante evaluations. When the CWD technology and the full cooperative system are available in large scale applications, more investigations will be needed and then the model could be empirically calibrated, also according to the observed driving behavior.

More developments can be carried out to improve the realism of the traffic simulator. For example, the speed in the other lanes is estimated according to the initial traffic density. In a further enhancement, for very high FEV

traffic level, the model could also consider that, during the time period, the density in the other lanes may change for both FEVs lane changing maneuvers and fluctuations of traditional “not electric” traffic. Even more complex scenarios with different vehicle types and related traffic flows could be analyzed. Furthermore, the model could be extended to flows of private cars, where the recharging needs should be related to the vehicle destinations, thus requiring the estimated demand data of detailed Origin/Destination matrixes.

## Acknowledgements

This study is partially supported by eCo-FEV project (Grant agreement no: 314411 - <http://www.eco-fev.eu/home.html>) and the authors would like to thank all the project partners for their useful support and suggestions on this subject.

## References

- Barceló J., Casas J. (2005), *Dynamic network simulation with AIMSUN*, in Simulation Approaches in Transportation Analysis, Vol.31, pp. 57-98, Springer, [http://dx.doi.org/10.1007/0-387-24109-4\\_3](http://dx.doi.org/10.1007/0-387-24109-4_3)
- Ben-Akiva M. , Gao S., Wei Z., Wen Y. (2012), *A dynamic traffic assignment model for highly congested urban networks*, in Transportation Research, Part C: Emerging Technologies, Vol.24, pp. 62-82, <http://dx.doi.org/10.1016/j.trc.2012.02.006>
- Boulanger A. G., Chu A. C., Maxx S., Waltz D.L. (2011), *Vehicle electrification: status and issues*, in Proceeding of the IEEE, Vol.99, Issue 6, pp. 1116-1138, <http://dx.doi.org/10.1109/JPROC.2011.2112750>
- Cascetta E. (2001), *Transportation systems engineering: theory and methods*, Kluwer
- Daganzo C.F. (1997), *Fundamentals of Transportation and Traffic Operations*, Pergamon
- Defflorio F., Guglielmi P., Pinna I., Castello L., Marfull S. (2013), *Modelling and Analysis of wireless “Charge While Driving” operations for Fully Electric Vehicles*, SIDT 2013 Scientific Seminar, Trieste (Italy), 18th October 2013. In press in Transportation Research Procedia (10.1016/j.trpro.2015.01.008)
- Drake J. S., Schofer J. L., May A. D. (1967), *A Statistical Analysis of Speed Density Hypotheses*, Third International Symposium on the Theory of Traffic Flow Proceedings, Elsevier North Holland, Inc., New York
- eCo-FEV (2013), *Use cases and requirements for an efficient cooperative platform*, Deliverable D200.1 of the eCo-FEV project, <http://www.eco-fev.eu/>
- ECSS (2009), *Space engineering – Verification*, ESA Requirements and Standards Division
- ETSI TR 102 638 V1.1.1 (2009-06), *Technical Report: Intelligent Transport Systems (ITS); Vehicular Communications; Basic Set of Applications; Definitions*
- Ezell S. (2010), *Explaining International IT Application leadership: Intelligent Transportation Systems*, The Information Technology & Innovation
- Farah H., Toledo T. (2010), *Passing behavior on two-lane highways*, in Transportation Research Part F: Traffic Psychology and Behaviour, Vol.13, Issue 6, pp. 355-364, <http://dx.doi.org/10.1016/j.trf.2010.07.003>
- Farah H. (2013), *Modeling drivers' passing duration and distance in a virtual environment*, in IATSS Research, Vol.37, Issue 1, pp. 61-67, <http://dx.doi.org/10.1016/j.iatssr.2013.03.001>
- Gutiérrez, J., García, J., Harbour, M. (1998), *Best-case analysis for improving the worst-case schedulability test for distributed hard real-time systems*, in Proceedings of the 10th Euromicro Workshop on Real-Time Systems, pp. 35-44, <http://dx.doi.org/10.1109/EMWRTS.1998.684945>
- Hoogendoorn S. P., Bovy P. H. L. (2001), *State-of-the-art of vehicular traffic flow modelling*, in Special Issue on Road Traffic Modelling and Control of the Journal of Systems and Control Engineering

INCOSE (2011), *Systems Engineering Handbook v. 3.2.2.*, INCOSE - TP - 2003 - 002 - 03.2.2

Johnson J., Chowdhury M., He Y., Taiber J. (2013), *Utilizing real time information transferring potentials to vehicles to improve the fast charging process in electric vehicles*, in Transportation research, Part C: Emerging Technologies, Vol.26, pp.352-366, <http://dx.doi.org/10.1016/j.trc.2012.10.009>

Kirsch D.A. (2000), *The electric vehicle and the burden of history*, Rutgers University press

Myers G. J., Badgett T., Sandler C. (2004), *The Art of Software Testing*, John Wiley and Sons Inc.

Palakon K., Wang Y., Imura T., Fujimoto H., Hon, Yoichi (2011), *Electric Vehicle Automatic Stop using Wireless Power Transfer Antennas*, in IECON 2011 - 37th Annual Conference on IEEE Industrial Electronics Society, pp. 3840-3845, <http://dx.doi.org/10.1109/IECON.2011.6119936>

Sun J., Chen S. (2013), *Dynamic speed guidance for active highway signal coordination: roadside against in-car strategies*, in Intelligent Transport Systems, IET, Vol.7, Issue 4, pp. 432-444, <http://dx.doi.org/10.1049/iet-its.2012.0084>